MedChemComm

Accepted Manuscript

ROYAL SOCIETY OF CHEMISTRY

www.rsc.org/medchemcomm

MedChemComm

RSCPublishing

CONCISE ARTICLE

Design, synthesis, and evaluation of semi-conservative mono-carbonyl analogs of curcumin as anti-inflammatory agents against lipopolysaccharide induced acute lung injury

Cite this: DOI: 10.1039/xoxxoooooox

Received ooth January 2012,
Accepted ooth January 2012

DOI: 10.1039/xoxxoooooox

www.rsc.org/

Lili Dong,[ab†] Suqing Zheng,[a†] Yali Zhang[a], Xin Jiang,[c] Jianzhang Wu,[a] Xiaoqin Zhang,[d] Xiaoou Shan,[b] Dandan Liang,[a] Shilong Ying,[a] Jianpeng Feng,[a*] and Guang Liang[a*]

Acute Lung Injury (ALI), one of severe diseases with high mortality, cannot be tackled by any effective therapies so far. Pro-inflammatory cytokines play an essential role in the pathogenesis of ALI. In order to discover novel anti-inflammatory agents against ALI, 37 Semi-conservative Mono-carbonyl Analogs of Curcumin (ScMACs) were designed, synthesized and screened for anti-inflammatory activities. The majority of these compounds exhibited remarkable inhibition of the expression of inflammatory cytokines in LPS-stimulated macrophages. Among them, compounds **6, 7, 10** and **18**, efficiently inhibited the secretion of TNF-α and IL-6 in a dose-dependent manner. The most potent analog, compound **6** prevented the LPS-induced elevation of inflammatory gene expression, and alleviated the lung inflammatory cells infiltration and histopathological changes *in vivo*. Therefore, the compound **6** is a potential lead for developing new anti-inflammatory candidate drug against LPS-induced ALI.

1. Introduction

Acute Lung Injury (ALI) is a critical disease characterized by the dysfunction of endothelial and epithelial barriers of the lung, the loss of alveolar-capillary membrane integrity, excessive transepithelial leukocyte migration, and overproduction of pro-inflammatory mediators.[1,2] ALI is usually caused by a variety of clinical disorders, such as pneumonia, aspiration of gastric contents, sepsis, major trauma and acute pancreatitis.[3] Despite the recent advances in many strategies for the treatment, ALI and its severe form acute respiratory distress syndrome (ARDS) still produce nearly 190,000 hospitalization and 74,500 deaths in the United States[4] since there are hardly any specific and effective therapies currently.[1,5] Therefore, a novel therapy is badly needed. Although the pathogenesis and genetic basis of ALI are not completely understood, abundant researches have confirmed that the inflammatory cytokines, chemokines and adhesion molecules play a major role in lung injury process.[6-8] The pro-inflammatory factor, such as tumour necrosis factor alpha (TNF-α)[9] and interleukin-6 (IL-6),[10] leads to the out-of-control inflammation followed by a series of pathologic responses.While adhesion molecules, such as intercellular cell adhesion molecule-1 (ICAM-1) and vascular cell adhesion molecule-1 (VCAM-1), mediate the adhesion between inflammatory cells and vascular endothelial cells.[11] Subsequently, a large amount of inflammatory cells, including neutrophils and macrophages, are flushed into lung tissues through blood vessels.[12] CD68, a specific macrophages marker, can be used to evaluate macrophage infiltration.[13] The increased infiltration of inflammatory cells further accelerates the production of inflammatory cytokines.[12] Thus, it may be a promising strategy to develop potential anti-inflammatory agents to down-regulate pro-inflammatory cytokines levels for treatment of patients with ALI.

Curcumin, a bioactive compound of the rhizome of *curcuma longa* and the major component of many Traditional Chinese Medicine, has drawn great interest due to its diverse biological activities, such as anti-inflammatory, antioxidant, anticarcinogenic, antimutagenic, anticoagulant, antifertility, antidiabetic, antibacterial, antifungal, antiviral, antifibrotic, antivenom, antiulcer, hypotensive, hypercholesterolemia, and cardioprotective activities,[14-19] while exhibiting no adverse side-effect or systemic toxicity.[20,21] Several reports demonstrated that curcumin could reduce severity of ALI.[22,23] Unfortunately, the clinical application of this biologically

versatile natural product is limited by its rapid plasma clearance, low bioavailability and unsatisfactory pharmacokinetics.[24,25] Considering that the β-diketone moiety in curcumin may be responsible for its instability *in vivo* and results in its rapid degradation,[26,27] our group has designed a series of Mono-carbonyl Analogs Curcumin (MACs) to overcome these drawbacks,[28-31] in which the β-diketone in curcumin is replaced by one simple ketone. These synthetic analogues show enhanced stability *in vitro* and improved pharmacokinetic profiles *in vivo*.[32] At the same time, many MACs possess strong anti-inflammatory properties, and some of them exhibit promising pharmacological effects and are subjected to the preclinical study. However, there are little research focused on protection effects of MACs against ALI.[33] In our perivous study about MACs, it was found that the presence of 3-methoxy group in aryl of curcumin was critical to the anti-inflammatory activity.[28,29] Our recent study about asymmetric MACs demonstrated that MACs with one 4-hydroxy-3-methoxyphenyl group in one side possessed the enhanced anti-inflammatory activity.[34] Therefore, we focus on the asymmetrical mono-carbonyl curcumin analogs with 4-hydroxy-3-methoxyphenyl group in one side, which are named as Semi-conservation Mono-carbonyl Analogs Curcumin (ScMACs) whereas retaining one aryl ring of curcumin (Fig. 1). Herein, a series of ScMACs were synthesized and evaluated in the bioassay. The most potent compound **6** was selected to test the effect on histopathological changes in lung and expression of inflammatory gene *in vitro* and *in vivo*. The results suggested that compound **6** had a great potential to serve as new anti-inflammatory agent for the treatment of ALI.

2. Results and discussion

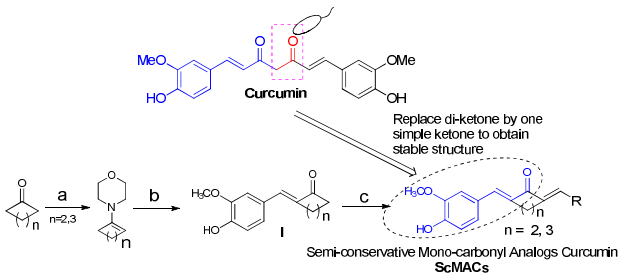

1: n=2, R= 3-indolyl;
2: n=2, R= naphthyl;
3: n=2, R= 3-pyrrolopyrimidine;
4: n=2, R= (2-fluoro-4-methoxy)phenyl;
5: n=2, R= 6-bromo-1,3-dihydroisobenzofuran-5-yl;
6: n=2, R= 5-bromo-3-indolyl;
7: n=2, R= 2,5-dimethylphenyl;
8: n=3, R= 2-fluorophenyl;
9: n=3, R= 2-bromophenyl, ;
10: n=3, R= (3-hydroxy-4-methoxy)phenyl;
11: n=3, R= 2,5-dimethoxyphenyl;
12: n=3, R= 3,4,5-trimethoxyphenyl;
13: n=3, R= (3-nitryl-4-chloro)phenyl;
14: n=3, R= 3,4-dihydroxyphenyl;
15: n=3, R= 4-chlorophenyl;
16: n=3, R= 6-bromo-1,3-dihydroisobenzofuran-5-yl;
17: n=3, R= (2-hydroxy-3-methoxy)phenyl;
18: n=3, R= (3-bromo-4-hydroxy)phenyl;
19: n=3, R= 2,4,6-trimethylphenyl;
20: n=3, R= (3-bromo-4-fluoro)phenyl;
21: n=3, R= 3,4-dimethoxyphenyl;
22: n=3, R= naphthyl;
23: n=3, R= 2,5-difluorophenyl;
24: n=3, R= 2-methoxyphenyl;
25: n=3, R= (3,5-dibromo-4-hydroxy)phenyl;
26: n=3, R= 2,4-dichlorophenyl;
27: n=3, R= 3-fluorophenyl;
28: n=3, R= 4-methoxyphenyl;
29: n=3, R= 2,4-dimethoxyphenyl;
30: n=3, R= 3,4-difluorophenyl;
31: n=3, R= 2,3-dichlorophenyl;
32: n=3, R= 4-hydroxyphenyl;
33: n=3, R= 2,3-dimethoxyphenyl;
34: n=3, R= 2-trifluoromethylphenyl;
35: n=3, R= 2,6-difluorophenyl;
36: n=3, R= 3,4-dichlorophenyl;
37: n=3, R= (2-ethoxyl-5-bromo)phenyl.

Figure 1. Structures and synthesis route of semi-conservative MACs compounds. Reagents and conditions: (a) Cyclopentanone or cyclohexanone, 4-methylbenzenesulfonic acid, cyclohexane, reflux, 4 h, 50%; (b) 4-hydroxy 3-methoxybenzaldehyde, EtOH, reflux, 4 h, 30-40%; (c) Different aldehydes, HCl gas, EtOH, 50-70 ^{o}C, 3-5 h, 3.4-36.8%.

2.1 Chemistry

The synthetic route and structures of the 37 ScMACs are shown in Figure 1. Intermediate **I** was prepared according to the previously reported methods.[34] Then, intermediate **I** reacted with corresponding aldehyde to obtain the target ScMACs. The chemical structures of all synthesized compounds were characterized by ^{1}H-NMR and ESI-MS. The general procedure and the characterization data are available in the experimental section.

2.2 Effects of semi-conservative mono-carbonyl analogs curcumins on cytokines production

RAW 264.7 macrophages, which are important tool cells for studying anti-inflammatory drugs, were pre-incubated with compounds (10 μM) for 30 min and subsequently treated with LPS (0.5 μg/mL) for 24 h. Culture medium was collected. The amount of IL-6 and TNF-α in media were detected through Enzyme-Linked Immunosorbant Assay (ELISA) and normalized by protein concentration of cells harvested in homologous cultures plates. The preliminary screening results of the anti-inflammatory activity of 37 ScMACs are shown in Figure 2A and 2B. Firstly, the levels of IL-6 and TNF-α were significantly increased after LPS treatment without ScMACs.

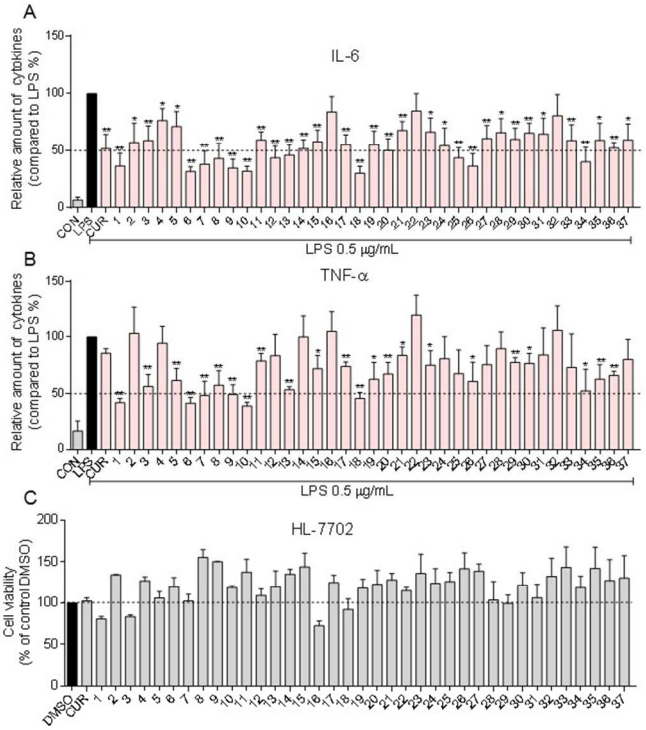

Figure 2. ScMACs showed anti-inflammatory activity and no cytotoxicity. (A) and (B): ScMACs inhibited LPS-induced IL-6 and TNF-α secretion in RAW 264.7 macrophages. Macrophages were plated at a density of 700000/plate for 24 h in 37 ^{o}C and 5% CO_2. Cells were pre-incubated with compounds (10 μM) for 30 min and subsequently treated with LPS (0.5 μg/mL) for 24 h. IL-6 (A) and TNF-α (B) levels in the culture medium were measured by ELISA and were normalized by the total protein. The results were presented as the percent of LPS control. Each bar represents mean ± SEM of three independent experiments. Statistical significance relative to LPS group was indicated, *p < 0.05, **P<0.01. (C) ScMACs showed no

toxicity to human hepatic cell. Human normal hepatic cell line, HL-7702, were plated at a density of 5000/plate in 96 well plates for 24 h in 37 °C and 5% CO_2. Then, cells were treated with compounds (10 μM) for 24 h. After that, the viability of cells was measured by MTT assay.

All ScMACs remarkably decreased LPS-induced IL-6 level (Figure 2A), while the expressions of TNF-α (Figure 2B) were inhibited by majority of ScMACs. It is worth mentioning that compounds **1**, **6**, **7**, **10**, and **18** exhibited great inhibition (>50%) against both IL-6 and TNF-α. Based on these results, we discussed the possible structure-activity relationship of ScMACs. Generally, the compounds with mono- or di-substituted aryl as R group are better than the compounds with tri-substituted R. The compounds with one electron-withdrawing substituent in R, especially in 2-position of R, exhibit high activities such as **8**, **9** and **34**. As for the compound with 3, 4-di-substituted R, the presence of two strong electron-withdrawing substitutes can bring good activity. Interestingly, ScMACs with one hydroxyl group in 3, 4-positions of R, such as **10** and **18**, show the best inhibitory-effect. When R is heterocyclic group or bicyclic group, indole group as R displays the best result based on the comparison as follows: **1** and **6** *vs*. **2**, **3** and **5**.

Furthermore, the cytotoxicity and safety of analogues were tested through MTT in the human normal hepatic cell line HL-7702 which is more sensitive than other cells on drugs cytotoxicity, after 24 hours treatment of the cells with compounds at a concentration of 10 □M. As shown in Figure 2C, the compounds **1**, **3**, **16**, and **18** display a little toxicity in hepatic cells, while most other compounds are relatively safe. Combining these data, compounds **6**, **7**, **10** and **18** were selected for the further evaluation of their dose-dependent inhibitory effects against LPS-induced IL-6 and TNF-α release.

2.3 Active compounds inhibit IL-6 and TNF-α secretion in a dose-dependent manner

Macrophages were pretreated with **6**, **7**, **10** and **18** in a series of concentrations (1, 5 and 10 μM) for 30 min and subsequently incubated with LPS (0.5 μg/mL) for 24 h. As shown in Figure 3, these compounds significantly decreased the TNF-α and IL-6 levels in a concentration-dependent manner. These results further indicated that these compounds had the potent anti-inflammatory activities.

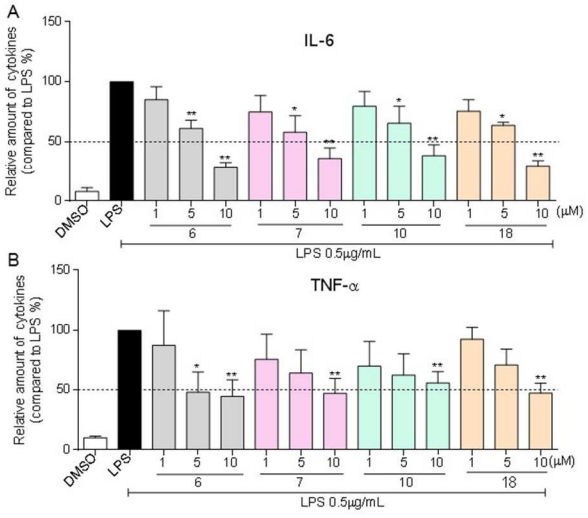

Figure 3. Compound **6**, **7**, **10**, and **18** induced down-regulation of LPS-induced IL-6 and TNF-α release in a dose-dependent manner. RAW 264.7 cells ($7x10^5$) were pretreated with 6 at indicated concentrations (0, 1, 5, and 10 μM) for 30 min. Then, Cells were incubated with LPS (0.5 μg/mL) for 24 h. Cytokine production in supernatants was measured by ELISA. Results are mean ± SD of at least four independent experiments. Statistical significance relative to LPS group was indicated, *P<0.05, **P<0.01.

2.4 Impact of compound 6 on LPS-mediated lung pathophysiologic change

Among the active compounds, compound **6** with the highest anti-inflammatory activity at 10 μM was selected to study the anti-inflammatory activity *in vivo*. It was evaluated in the rats with ALI induced by intratracheal instillation of LPS, which resembles many characteristics of human ALI.[35] Firstly, the rats were orally pretreated with or without compound **6** (20 mg/kg/day) for 7 days. Then, the LPS and LPS + **6** group rats were intratracheally instilled with LPS to induce acute lung injury, while rats from control group were treated by the physiological saline without LPS. Six hours after LPS perfusion, the rats were euthanized. The bronchoalveolar lavage fluid (BALF) and lungs tissues were collected. The total protein concentration, the numbers of neutrophils and the amount of TNF-α in BALF and the Wet/Dry ratio of lung tissue were evaluated. The results in Figure 4 indicated that the compound **6** decreased the elevation of protein concentration (Figure 4A), numbers of neutrophils (Figure 4B) and amount of TNF-α (Figure 4C) in BALF as well as the Wet/Dry ratio of lung tissue (Figure 4D) induced by LPS. These results suggested that the administrations of compound **6** reduced the LPS-mediated cellular infiltration and pulmonary edema.

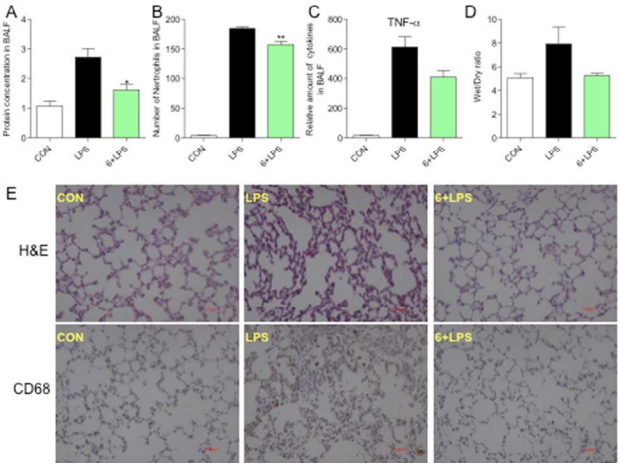

Figure 4. Compound **6** attenuated lung pathophysiologic changes in LPS-challenged rats. A-D: Effects of **6** on the total protein concentration (A), number of neutrophils in BALF (B), amount of TNF-α in BALF (C), and the lung W/D ratio (D) of LPS-induced ALI rats. E: Effects of **6** on histopathological change in lung tissue in ALI model induced by LPS (H&E staining and CD68 immunohistochemistical staining). *P<0.05, **P<0.01.

To evaluate the histological changes in LPS-treated rats, lung sections were also colorated with Hematoxylin and Eosin (H&E) stain and Cluster of Differentiation 68 (CD68) immunohistochemistical stain. In the control groups, lung tissues showed a normal structure and clear pulmonary alveoli (Figure 4E, control). In contrast, lung tissues were damaged in LPS group (Figure 4E, LPS), manifesting as infiltration of inflammatory cell, thickening of alveolar wall, and lessening of alveolar space. These destruction changes of lung were significantly attenuated by the pretreatment of compound **6**. Similarly, compound **6** reduced the LPS-induced macrophages infiltration in lung tissues. The

histological changes after pretreatment of compound **6** demonstrate that it has protective effect against LPS-induced ALI.

2.5 Effect of compound 6 in the expression of inflammatory genes in vivo and in vitro

As compound **6** showed excellent anti-inflammatory effects *in vitro*, here we further evaluated its effects on gene expression of inflammatory cytokines in lung tissue. As shown in Figure 5, the mRNA expressions of TNF-α, IL-6, IL-1β, COX-2, ICAM-1, and VCAM-1 were suppressed (38.4%, 92.9%, 39.2%, 77.3%, 74.1% and 52.9% inhibition, respectively) in the lung tissue of **6**-pretreated rats compared with LPS-treated group. At the same time, the levels of inflammatory cytokines genes in cultured human lung epithelial cells BEAS-2B, which were used to further validate the anti-inflammatory effects, were also measured using real-time qPCR. The results illustrated in Figure 6 were consistent with results above in the lung tissue. The compound **6** inhibited the LPS-elicited release of inflammatory genes, including TNF-α (64.5%), IL-6 (30.0%), IL-1β (55.6%), and COX-2 (64.9%) in cell. Therefore, the compound **6** is able to inhibit the expressions of inflammatory genes both *in vivo* and *in vitro*. It is consistent with the inflammatory cytokines changes.

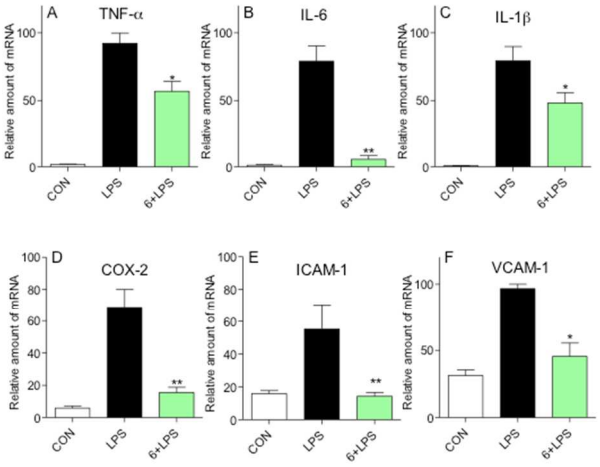

Figure 5. Effects of **6** on the expression of inflammatory genes on lung tissue. The levels of TNF-α (A), B: IL-6 (B), IL-1β (C), COX-2 (D), ICAM-1 (E), VCAM-1 (F) was analyzed by mRNA assay. *P<0.05, **P<0.01.

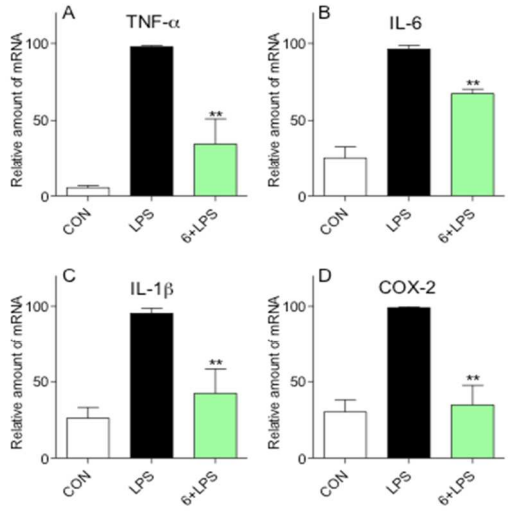

Figure 6. Compound **6** inhibited the expression of inflammatory genes in the human lung epithelial cells analyzed by mRNA assay. A: TNF-α, B: IL-6, C: IL-1β, D: COX-2. The results were presented as the percent of LPS control. Each bar represents mean ± SEM of three independent experiments. Statistical significance relative to LPS group was indicated, *p < 0.05, **P<0.01.

above and reveals that compound **6** may have a protective effect on LPS-induced acute lung injury through its anti-inflammatory activity

3. Conclusions

In the present study, we synthesized 37 ScMACs and evaluated their anti-inflammatory activities in LPS-mediated macrophages. Most of these compounds inhibit the LPS-induced IL-6 and TNF-α release. Meanwhile, the toxicity experiments show that majority of them are safe in human normal hepatic cell line, HL-7702. The preliminary SAR analysis was conducted to outline the effects of the structures of ScMACs on their pharmacological activity. Four selected active compounds, including **6, 7, 10**, and 1**8**, efficiently inhibit the secretion of IL-6 and TNF-α in a dose-dependent manner. The most potent compound **6** was evaluated *in vivo*. It significantly attenuates the pathophysiologic changes induced by LPS administration. In addition, the compound **6** efficiently suppresses the increase of inflammatory cytokines gene expression induced by LPS *in vivo* and *in vitro*. That may be the reason why the compound **6** can inhibit LPS-induced IL-6 and TNF-α secretion and decrease the damage of ALI. These results demonstrate ScMACs may be promising candidates for the treatment of ALI. Further studies involving mechanism investigation and lead optimization based on the structure of **6** are underway in our group.

4. Experimental Section

4.1 Chemistry

In general, reagents, solvents, and other chemicals were used as purchased without further purification. All reagents for synthesis were obtained from Sigma Aldrich and Fluka. Thin-layer chromatography (TLC) was performed on Kieselgel 60 F_{254} plates and flash column chromatography (medium pressure liquid chromatography) purifications were carried out using Merck silica gel 60 (230-400 mesh ASTM) (Merck KGaA, Darmstadt, Germany). Melting points were determined on a Fisher-Johns melting apparatus and were uncorrected. ^{1}H NMR spectra were recorded on a Bruker 600 MHz instruments. The chemical shifts were presented in terms of parts per million with TMS as the internal reference. Electron-spray ionization mass spectra in positive mode (ESI-MS) data were recorded on a Bruker Esquire 3000t spectrometer. All general chemicals were purchased directly from commercial sources and were used as supplied.

4.1.1 General procedure

All compound **1-37** were synthesized with a similar method previously developed by our group.[34] To a solution of cyclopentanone or cyclohexanone (10 mmol) and *p*-toluenesulfonic acid (100 mg, 0.58 mmol, 5.8%) in cyclohexane (20 mL) was added morpholine (20 mmol). The mixture was heated to reflux at 90 °C for 4 h. After cooled to rt, this solution was washed with water, dried and concentrated to give crude enamine as light yellow liquid, which was mixed with vanillin (10 mmol) in ethanol (15 mL). The resulted

solution was heated to reflux at 90 °C for 4 h. Since the TLC monitoring showed complete conversion, saturated NaCl was added into this solution and then concentrated *in vacuo*. The residue was purified by flash column chromatography on silica gel eluting with hexane: ethyl ester = 1:1 to give intermediate **I**. The mixture of intermediate **I** and corresponding aldehyde (1:1) in ethanol (15 mL) was slowly passed through HCl gas at 50-70 °C for 3-5 h. Once the reaction was complete (as evident by TLC), H_2O (15 mL) and ethyl ester (20 mL) were poured to this reaction solution. Organic phase was concentrated and subsequently purified by flash column chromatography to afford target product **1-37**. The yield of last step was calculated. ^{1}H-NMR spectrum of known compound **32** was consistent with that in the literature.[36] The structures of other synthesized compounds were characterized by ^{1}H-NMR and MS.

4.1.2 Compound

(2*E*,5*E*)-2-[(1H-indol-2-yl)methylene]-5-(4-hydroxy-3-methoxybenzyli dene)cyclopentanone (1): Yellow powder, 6.7% yield, mp 257.6-259.1°C. ^{1}H-NMR (d_6-DMSO) δ: 7.846 (d, J = 7.8 Hz, 1H, H-7′), 7.813 (d, J = 3.0 Hz, 1H, H-4′), 7.792 (s, 1H, β′-H), 7.475 (d, J = 8.4 Hz, 1H, H-6), 7.309 (s, 1H, β-H), 7.239 (s, 1H, H-2), 7.212 (t, J = 7.2 Hz, 1H, H-5), 7.160 (t, J = 7.8 Hz, 2H, H-5′, H-6′), 6.875 (d, J = 8.4 Hz, 1H, H-3′), 3.832 (s, 3H, 3-OCH_3), 2.926-3.094 (m, 4H, 3″-CH_2, 4″-CH_2). ESI-MS m/z: 346.2 $(M+1)^+$, calcd for $C_{22}H_{19}NO_3$: 345.1.

(2*E*,5*E*)-2-(4-Hydroxy-3-methoxybenzylidene)-5-(naphthalen-2-ylmethylene)cyclopentanone (2): Yellow powder, 3.4% yield, mp 198.3-201.3°C. ^{1}H-NMR (d_6-DMSO) δ: 8.241 (s, 1H, H-1′), 7.979-8.105 (m, 2H, H-5′, H-8′), 7.939 (t, J = 9.0 Hz, 1H, H-4′), 7.797 (d, J = 8.4 Hz, 1H, H-3′), 7.560 (q, J = 7.8 Hz, 4H, β-H, β′-H, H-6′, H-7′), 7.268 (s, 1H, H-2), 7.191 (d, J = 8.4 Hz, 1H, H-6), 6.893 (d, J = 8.4 Hz, 1H, H-5), 3.835 (s, 3H, 3-OCH_3), 3.107-3.216 (m, 4H, 3″-CH_2, 4″-CH_2). ESI-MS m/z: 357.1 $(M+1)^+$, calcd for $C_{24}H_{20}O_3$: 356.1.

(2*E*,5*E*)-2-{(1H-pyrrolo[2,3-b]pyridin-3-yl)methylene}-5-(4-hydroxy-3-methoxybenzylidene)cyclopentanone (3): Reddish brown powder, 5.1% yield, mp 263.1-265.6°C. ^{1}H-NMR (d_6-DMSO) δ: 8.339 (t, J = 7.8 Hz, 2H, H-4′, H-6′), 7.916 (s, 1H, β′-H), 7.760 (s, 1H, β-H), 7.342 (s, 1H, H-5′), 7.260 (s, 1H, H-2), 7.168-7.226 (m, 2H, H-2′, H-6), 6.892 (d, J = 7.8 Hz, 1H, H-5), 3.847 (s, 3H, 3-OCH_3,), 3.103 (d, J = 5.4 Hz, 2H, 3″-CH_2), 2.978 (d, J = 5.4 Hz, 2H, 4″-CH_2). ESI-MS m/z: 347.1 $(M+1)^+$, calcd for $C_{21}H_{18}N_2O_3$: 346.1.

(2*E*,5*E*)-2-(2-Fluoro-4-methoxybenzylidene)-5-(4-hydroxy-3-methoxybenzylidene)cyclopentanone (4): Green powder, 4.6% yield, mp 174.8-177.5°C. ^{1}H-NMR (d_6-DMSO) δ: 7.690 (t, J = 9.0 Hz, 1H, H-6′), 7.474 (s, 1H, β′-H), 7.397 (s, 1H, β-H), 7.358 (s, 1H, H-3′), 7.186 (d, J = 1.8 Hz, 1H, H-2), 7.164 (d, J = 8.4 Hz, 1H, H-5), 6.988 (dd, J_1 = 2.4 Hz, J_2 = 9.0 Hz, 1H, H-6), 6.926 (dd, J_1 = 2.4 Hz, J_2 = 8.4 Hz, 1H, H-5′), 3.838 (s, 6H, 3-OCH_3, 4′-OCH_3), 3.023-3.068 (m, 4H, 3″-CH_2, 4″-CH_2). ESI-MS m/z: 355.1 $(M+1)^+$, calcd for $C_{21}H_{19}FO_4$: 354.1.

(2*E*,5*E*)-2-{(6-Bromobenzo[d][1,3]dioxol-5-yl)methylene}-5-(4-hydroxy-3-methoxybenzylidene)cyclopentanone (5): Orange yellow powder, 17.9% yield, mp 247.3-250.1°C. ^{1}H-NMR (d_6-DMSO) δ: 7.535 (s, 1H, β′-H), 7.404 (s, 1H, β-H), 7.394 (s, 1H, H-2), 7.280 (s, 1H, H-5′), 7.179 (d, J = 9.0 Hz, 1H, H-6), 6.892 (d, J = 8.4 Hz, 1H, H-5), 6.160 (s, 1H, H-2′), 6.110 (s, 2H, -OCH_2O-), 3.835 (s, 3H, 3-OCH_3), 3.029 (s, 4H, 3″-CH_2, 4″-CH_2). ESI-MS m/z: 429.0 $(M+1)^+$, calcd for $C_{21}H_{17}BrO_5$: 428.0.

(2*E*,5*E*)-2-[(5-Bromo-1H-indol-3-yl)methylene]-5-(4-hydroxy-3-methoxybenzylidene)cyclopentanone (6): Orange powder, 15.1% yield, mp 272.4-275.0°C. ^{1}H-NMR (d_6-DMSO) δ: 8.071 (s, 1H, H-2′), 7.872 (s, 1H, β′-H), 7.755 (s, 1H, β-H), 7.456 (d, J = 8.4 Hz, 1H, H-6′), 7.336 (t, J = 6.6 Hz, 2H, H-2, H-6), 7.258 (s, 1H, H-4′), 7.173 (d, J = 8.4 Hz, 1H, H-7′), 6.891 (d, J = 8.4 Hz, 1H, H-5), 3.847 (s, 3H, 3-OCH_3), 2.934-3.104 (m, 4H, 3″-CH_2, 4″-CH_2). ESI-MS m/z: 423.7 $(M+1)^+$, calcd for $C_{22}H_{18}BrNO_3$: 423.0.

(2*E*,5*E*)-2-(2,5-Dimethylbenzylidene)-5-(4-hydroxy-3-methoxybenzylidene)cyclopentanone (7): Orange powder, 34.2% yield, mp 224.7-227.5°C. ^{1}H-NMR (d_6-DMSO) δ: 8.072 (s, 1H, β′-H), 7.755 (s, 1H, β-H), 7.546 (s, 1H, H-2), 7.456 (d, J = 8.4 Hz, 1H, H-6), 7.410 (s, 1H, H-6′), 7.116 (d, J = 7.8 Hz, 2H, H-3′, H-5), 6.894 (dd, J_1 = 2.4′ Hz, J_2 = 8.4 Hz, 1H, H-4′), 3.825 (s, 3H, 3-OCH_3), 2.934-3.104 (m, 4H, 3″-CH_2, 4″-CH_2), 2.339 (s, 3H, 2′-CH_3), 2.322 (s, 3H, 5′-CH_3). ESI-MS m/z: 335.0 $(M+1)^+$, calcd for $C_{22}H_{22}O_3$: 334.2.

(2*E*,6*E*)-2-(2-Fluorobenzylidene)-6-(4-hydroxy-3-methoxybenzylidene)cyclohexanone (8): Yellow powder, 20.4% yield, mp 158.5-161.6°C. ^{1}H-NMR (d_6-DMSO) δ: 7.663-7.742 (m, 2H, β′-H, H-4′), 7.559 (s, 2H, β-H, H-6′), 7.113 (d, J = 1.8 Hz, 2H, H-3′, H-5′), 7.031 (dd, J_1 = 1.8 Hz, J_2 = 8.4 Hz, 2H, H-5, H-6), 6.856 (s, 1H, H-2), 3.810 (s, 3H, 3-OCH_3), 2.890 (t, J = 5.4 Hz, 4H, 3″-CH_2, 5″-CH_2), 1.677-1.747 (m, 2H, 5″-CH_2). ESI-MS m/z: 338.7 $(M+1)^+$, calcd for $C_{21}H_{19}FO_3$: 338.1.

(2*E*,6*E*)-2-(2-Bromobenzylidene)-6-(4-hydroxy-3-methoxybenzylidene)cyclohexanone (9): Brown powder, 3.8% yield, mp 157.6-160.2°C. ^{1}H-NMR (d_6-DMSO) δ: 7.561 (s, 3H, β-H, β′-H, H-3′), 7.115 (d, J = 1.2 Hz, 2H, H-2, H-6′), 7.033 (dd, J_1 = 1.2 Hz, J_2 = 7.8 Hz, 2H, H-4′, H-5′), 6.850 (d, J = 7.8 Hz, 2H, H-5, H-6), 3.811 (s, 3H, 3-OCH_3), 2.894 (t, J = 5.4 Hz, 4H, 3″-CH_2, 5″-CH_2), 1.708-1.747 (m, 2H, 4″-CH_2). ESI-MS m/z: 399.0 $(M+1)^+$, calcd for $C_{21}H_{19}BrO_3$: 398.1.

(2*E*,6*E*)-2-(4-Hydroxy-3-methoxybenzylidene)-6-(3-hydroxy-4-methoxybenzylidene)cyclohexanone (10): Brown yellow powder, 9.8% yield, mp 140.5-142.7°C. ^{1}H-NMR (d_6-DMSO) δ: 7.544 (s, 2H, β-H, β′-H), 7.098 (s, 2H, H-2, H-2′), 7.008 (t, J = 7.8 Hz, 3H, H-5, H-6, H-6′), 6.833 (d, J = 8.4 Hz, 1H, H-5′), 3.795 (s, 6H, 3-OCH_3, 4′-OCH_3), 2.873 (d, J = 5.4 Hz, 4H, 3″-CH_2, 5″-CH_2), 1.709 (t, J = 5.4 Hz, 2H, 4″-CH_2). ESI-MS m/z: 367.0 $(M+1)^+$, calcd for $C_{22}H_{22}O_5$: 366.1.

(2*E*,6*E*)-2-(2,5-Dimethoxybenzylidene)-6-(4-hydroxy-3-methoxybenzylidene)cyclohexanone (11): Yellow powder, 5.3% yield, mp 113.2-115.8°C. ^{1}H-NMR (d_6-DMSO) δ: 7.722 (s, 1H, β'-H), 7.572 (s, 1H, β-H), 7.298 (s, 1H, H-6), 7.127 (d, J = 1.8 Hz, 1H, H-2), 7.052 (d, J = 8.4 Hz, 1H, H-5), 7.000 (d, J = 9.0 Hz, 1H, H-3′), 6.835 (dd, J_1 = 1.2 Hz, J_2 = 8.4 Hz, 1H, H-4′), 6.635 (s, 1H, H-6′), 3.733 (s, 3H, 3-OCH_3), 3.701 (s, 3H, 2′-OCH_3), 3.678 (s, 3H, 5′-OCH_3), 2.876-2.911 (m, 4H, 3″-CH_2, 5″-CH_2), 1.680-1.720 (m, 2H, 4″-CH_2). ESI-MS m/z: 381.0 $(M+1)^+$, calcd for $C_{23}H_{24}O_5$: 380.2.

(2*E*,6*E*)-2-(4-Hydroxy-3-methoxybenzylidene)-6-(3,4,5-trimethoxybenzylidene)cyclohexanone (12): Yellow powder, 5.4% yield, mp 142.8-144.1°C. ^{1}H-NMR (d_6-DMSO) δ: 7.578 (s, 2H, β-H, β′-H), 7.130 (s, 1H, H-2), 7.054 (d, J = 8.4 Hz, 1H, H-6), 6.856 (d, J

= 7.8 Hz, 1H, H-5), 6.836 (s, 2H, H-2′, H-6′), 3.815 (s, 9H, 3′,4′,5′-OCH_3), 3.701 (s, 3H, 3-OCH_3), 2.896-2.941 (m, 4H, 3″-CH_2, 5″-CH_2), 1.711-1.751 (m, 2H, 4″-CH_2). ESI-MS m/z: 411.0 $(M+1)^+$, calcd for $C_{24}H_{26}O_6$: 410.2.

(2*E*,6*E*)-2-(4-Chloro-3-nitrobenzylidene)-6-(4-hydroxy-3-methoxybenzylidene)cyclohexanone (13): Yellow powder, 10.0% yield, mp 171.7-173.6°C. ^{1}H-NMR (d_6-DMSO) δ: 7.555 (s, 2H, H-2′, *β*′-H), 7.108 (s, 2H, *β*-H, H-2), 7.030 (d, *J* = 8.4 Hz, 2H, H-5′, H-6’), 6.847 (d, *J* = 7.8 Hz, 2H, H-5, H-6), 3.807 (s, 3H, 3-OCH_3), 2.889 (t, *J* = 5.4 Hz, 4H, 3″-CH_2, 5″-CH_2), 1.722 (t, *J* = 5.4 Hz, 2H, 4″-CH_2). ESI-MS m/z: 399.9 $(M+1)^+$, calcd for $C_{21}H_{18}ClNO_5$: 399.1.

(2*E*,6*E*)-2-(3,4-Dihydroxybenzylidene)-6-(4-hydroxy-3-methoxybenzylidene)cyclohexanone (14): Yellow powder, 18.5% yield, mp 132.8-134.9°C. ^{1}H-NMR (d_6-DMSO) δ: 7.561 (s, 2H, *β*-H, *β*′-H), 7.115 (d, *J* = 1.8 Hz, 2H, H-2, H-2′), 7.034 (dd, J_1 = 1.8 Hz, J_2 = 8.4 Hz, 2H, H-6, H-6′), 6.849 (d, *J* = 8.4 Hz, 2H, H-5′, H-5), 3.811 (s, 3H, 3-OCH_3), 2.894 (t, *J* = 5.4 Hz, 4H, 3″-CH_2, 5″-CH_2), 1.707-1.747 (m, 2H, 4″-CH_2). ESI-MS m/z: 352.9 $(M+1)^+$, calcd for $C_{21}H_{20}O_5$: 352.1.

(2*E*,6*E*)-2-(4-Chlorobenzylidene)-6-(4-hydroxy-3-methoxybenzylidene)cyclohexanone (15): Earthy yellow powder, 17.7% yield, mp 158.9-161.3°C. ^{1}H-NMR (d_6-DMSO) δ: 9.521 (d, *J* = 8.4 Hz, 2H, H-2′, H-6′), 7.561 (s, 2H, *β*-H, *β*′-H), 7.115 (d, *J* = 8.4 Hz, 2H, H-3′, H-5′), 7.032 (dd, J_1 = 1.2 Hz, J_2 = 8.4 Hz, 2H, H-2, H-6), 6.850 (s, *J* = 7.8 Hz, 1H, H-5), 3.811 (s, 3H, 3-OCH_3), 2.892 (t, *J* = 5.4 Hz, 4H, 3″-CH_2, 5″-CH_2), 1.707-1.747 (m, 2H, 4″-CH_2). ESI-MS m/z: 354.8 $(M+1)^+$, calcd for $C_{21}H_{19}ClO_3$: 354.1.

(2*E*,6*E*)-2-{(6-Bromobenzo[d][1,3]dioxol-5-yl)methylene}-6-(4-hydroxy-3-methoxybenzylidene)cyclohexanone (16): Yellow green powder, 17.8% yield, mp 160.2-162.7°C. ^{1}H-NMR (d_6-DMSO) δ: 7.561 (s, 1H, *β*′-H), 7.404 (s, 1H, *β*-H), 7.394 (s, 1H, H-2), 7.280 (s, 1H, H-5′), 7.250 (s, 1H, H-2′), 7.180 (d, *J* = 9.0 Hz, 1H, H-6), 7.892 (d, *J* = 8.4 Hz, 1H, H-5), 6.160 (s, 2H, -OCH_2O-), 3.828 (s, 3H, 3-OCH_3), 2.679-2.901 (m, 4H, 3″-CH_2, 5″-CH_2), 1.672-1.856 (m, 2H, 4″-CH_2). ESI-MS m/z: 442.9 $(M+1)^+$, calcd for $C_{21}H_{19}BrO_5$: 442.0.

(2*E*,6*E*)-2-(2-Hydroxy-3-methoxybenzylidene)-6-(4-hydroxy-3-methoxybenzylidene)cyclohexanone (17): Yellow powder, 9.0% yield, mp 159.8-162.4°C. ^{1}H-NMR (d_6-DMSO) δ: 7.556 (s, 2H, *β*-H, *β*′-H), 7.109 (d, *J* = 1.2 Hz, 2H, H-2, H-6′), 7.031 (dd, J_1 = 1.2 Hz, J_2 = 8.4 Hz, 2H, H-5′, H-6), 6.848 (d, *J* = 8.4 Hz, 2H, H-5, H-4′), 3.807 (s, 6H, 3-OCH_3, 3′-OCH_3), 2.889 (t, *J* = 5.4 Hz, 4H, 3″-CH_2, 5″-CH_2), 1.703-1.744 (m, 2H, 4″-CH_2). ESI-MS m/z: 367.0 $(M+1)^+$, calcd for $C_{22}H_{22}O_5$: 366.1.

(2*E*,6*E*)-2-(3-Bromo-4-hydroxybenzylidene)-6-(4-hydroxy-3-methoxybenzylidene)cyclohexanone (18): Orange yellow powder, 11.6% yield, mp 165.8-166.9°C. ^{1}H-NMR (d_6-DMSO) δ: 7.678 (s, 1H, H-2′), 7.556 (s, 2H, *β*-H, *β*′-H), 7.408 (d, *J* = 8.4 Hz, 1H, H-6′), 7.023 (t, *J* = 7.8 Hz, 3H, H-5, H-6, H-5′), 6.854 (s, 1H, H-2), 3.807 (s, 3H, 3-OCH_3), 2.832-2.897 (m, 4H, 3″-CH_2, 5″-CH_2), 1.722 (brs, 2H, 4″-CH_2). ESI-MS m/z: 414.7 $(M+1)^+$, calcd for $C_{21}H_{19}BrO_4$: 414.0.

(2*E*,6*E*)-2-(4-Hydroxy-3-methoxybenzylidene)-6-(2,4,6-trimethylbenzylidene)cyclohexanone (19): Yellow powder, 18.8% yield, mp 174.9-178.0°C. ^{1}H-NMR (d_6-DMSO) δ: 7.558 (s, 2H, *β*-H, *β*′-H), 7.111 (d, *J* = 1.8 Hz, 1H, H-2), 7.030 (dd, J_1 = 1.8 Hz, J_2 = 8.4 Hz, 2H, H-5, H-6), 6.855 (s, 1H, H-3′), 6.842 (s, 1H, H-5′), 3.809 (s, 3H, 3-OCH_3), 2.891 (t, *J* = 5.4 Hz, 4H, 3″-CH_2, 5″-CH_2), 2.500 (s, 9H, 2′,4′,6′-CH_3), 1.704-1.745 (m, 2H, 4″-CH_2). ESI-MS m/z: 362.8 $(M+1)^+$, calcd for $C_{24}H_{26}O_3$: 362.2.

(2*E*,6*E*)-2-(3-Bromo-4-fluorobenzylidene)-6-(4-hydroxy-3-methoxybenzylidene)cyclohexanone (20): Brown yellow powder, 36.8% yield, mp 166.9-169.1°C. ^{1}H-NMR (d_6-DMSO) δ: 7.662 (s, 1H, *β*′-H), 7.558 (s, 1H, H-2′), 7.112 (s, 2H, *β*-H, H-2), 7.031 (d, *J* = 7.8 Hz, 2H, H-6’, H-6), 6.848 (d, *J* = 7.8 Hz, 2H, H-5, H-5’), 3.809 (s, 3H, 3-OCH_3), 2.891 (t, *J* = 5.4 Hz, 4H, 3″-CH_2, 5″-CH_2), 1.705-1.734 (m, 2H, 4″-CH_2). ESI-MS m/z: 416.8 $(M+1)^+$, calcd for $C_{21}H_{18}BrFO_3$: 416.0.

(2*E*,6*E*)-2-(3,4-Dimethoxybenzylidene)-6-(4-hydroxy-3-methoxybenzylidene)cyclohexanone (21): Yellow powder, 5.3% yield, mp 126.8-129.5°C. ^{1}H-NMR (d_6-DMSO) δ: 7.578 (s, 2H, *β*-H, *β*’-H), 7.104-7.144 (m, 4H, H-2, H-6, H-2′, H-6′), 7.020 (d, *J* = 9.0 Hz, 2H, H-5, H-5′), 3.785 (s, 9H, 3′, 4′ -OCH_3, 3-OCH_3), 2.899 (t, *J* = 5.4 Hz, 4H, 3″-CH_2, 5″-CH_2), 1.700-1.740 (m, 2H, 4″-CH_2). ESI-MS m/z: 380.5 $(M)^+$, calcd for $C_{23}H_{24}O_5$: 380.2.

(2*E*,6*E*)-2-(4-Hydroxy-3-methoxybenzylidene)-6-(naphthalen-2-ylmethylene)cyclohexanone (22): Yellow powder, 8.1% yield, mp 177.3-178.9°C. ^{1}H-NMR (d_6-DMSO) δ: 8.101 (s, 1H, H-1′), 7.959-8.101 (m, 2H, H-5′, H-8′), 7.941 (t, *J* = 9.0 Hz, 1H, H-4′), 7.769 (s, 1H, *β*’-H), 7.660 (d, *J* = 8.4 Hz, 1H, H-3′), 7.621 (s, 1H, *β*-H), 7.562 (t, *J* = 8.4 Hz, H-6’, H-7′), 7.150 (s, 1H, H-2), 7.073 (dd, J_1 = 1.8 Hz, J_2 = 8.4 Hz, 1H, H-6), 6.868 (d, *J* = 7.8 Hz, 1H, H-5), 3.825 (s, 3H, 3-OCH_3), 2.927-3.105 (m, 4H, 3″-CH_2, 5″-CH_2), 1.740-1.781 (m, 2H, 4″-CH_2). ESI-MS m/z: 371.1 $(M+1)^+$, calcd for $C_{25}H_{22}O_3$: 370.2.

(2*E*,6*E*)-2-(2,5-Difluorobenzylidene)-6-(4-hydroxy-3-methoxybenzylidene)cyclohexanone (23): Yellow brown powder, 23.9% yield, mp 168.3-171.1°C. ^{1}H-NMR (d_6-DMSO) δ: 7.559 (s, 2H, *β*-H, *β*′-H), 7.114 (d, *J* = 1.8 Hz, 2H, H-6′, H-2), 7.033 (dd, J_1 = 1.8 Hz, J_2 = 8.4 Hz, 2H, H-6, H-4′), 6.849 (d, *J* = 8.4 Hz, 2H, H-5, H-3′), 3.810 (s, 3H, 3-OCH_3), 2.892 (t, *J* = 4.8 Hz, 4H, 3″-CH_2, 5″-CH_2), 1.706-1.746 (m, 2H, 4’’-CH_2). ESI-MS m/z: 357.1 $(M+1)^+$, calcd for $C_{21}H_{18}F_2O_3$: 356.4.

(2*E*,6*E*)-2-(4-Hydroxy-3-methoxybenzylidene)-6-(2-methoxybenzylidene)cyclohexanone (24): Yellow powder, 10.2% yield, mp 140.1-142.8°C. ^{1}H-NMR (d_6-DMSO) δ: 7.768 (s, 1H, H-6′), 7.575 (s, 1H, *β*′-H), 7.356-7.389 (m, 2H, H-4′, *β*-H), 7.128 (s, 1H, H-2), 7.076 (d, *J* = 8.4 Hz, 1H, H-6), 7.050 (d, *J* = 6.6 Hz, 1H, H-5), 7.002 (t, *J* = 7.8 Hz, 1H, H-5′), 6.856 (d, *J* = 8.4 Hz, 1H, H-3′), 3.833 (s, 3H, 2′-OCH_3), 3.815 (s, 3H, 3-OCH_3), 2.765-2.916 (m, 4H, 3″-CH_2, 5″-CH_2), 1.675-1.716 (m, 2H, 4″-CH_2). ESI-MS m/z: 351.1 $(M+1)^+$, calcd for $C_{22}H_{22}O_4$: 350.2.

(2*E*,6*E*)-2-(3,5-Dibromo-4-hydroxybenzylidene)-6-(4-hydroxy-3-methoxybenzylidene)cyclohexanone (25): Yellow powder, 3.4% yield, mp 170.3-172.5°C. ^{1}H-NMR (d_6-DMSO) δ: 7.561 (s, 2H, H-2′, H-6′), 7.115 (s, 2H, *β*-H, *β*′-H), 7.034 (dd, J_1 = 1.8 Hz, J_2 = 8.4 Hz, 2H, H-2, H-6), 6.856 (d, *J* = 7.8 Hz, 1H, H-5), 3.812 (s, 3H, 3-OCH_3), 2.894 (t, *J* = 5.4 Hz, 4H, 3″-CH_2, 5″-CH_2), 1.707-1.747 (m, 2H, 4″-CH_2). ESI-MS m/z: 492.8 $(M+1)^+$, calcd for $C_{21}H_{18}Br_2O_4$: 492.0.

(2*E*,6*E*)-2-(2,4-Dichlorobenzylidene)-6-(4-hydroxy-3-methoxybenzylidene)cyclohexanone (26): Yellow powder, 8.6% yield, mp 169.2-171.4°C. ^{1}H-NMR (d_6-DMSO) δ: 7.561 (s, 2H, *β*-H, *β*′-H), 7.115 (d, *J* = 1.2 Hz, 2H, H-2, H-3′), 7.033 (d, *J* = 8.4 Hz, 2H,

H-5′, H-6′), 6.850 (d, J = 8.4 Hz, 2H, H-5, H-6), 3.812 (s, 3H, 3-OCH_3), 2.893 (t, J = 5.4 Hz, 4H, 3″-CH_2, 5″-CH_2), 1.706-1.747 (m, 2H, 4″-CH_2). ESI-MS m/z: 387.9 $(M)^+$, calcd for $C_{21}H_{18}Cl_2O_3$: 388.1.

(2*E*,6*E*)-2-(3-Fluorobenzylidene)-6-(4-hydroxy-3-methoxybenzylidene)cyclohexanone (27):Orange yellow powder, 25.7% yield, mp 168.8-171.0°C. ^{1}H-NMR (d_6-DMSO) δ: 7.561 (s, 3H, β-H, β'-H, H-6′), 7.115 (d, J = 1.2 Hz, 2H, H-2, H-5′), 7.032 (dd, J_1 = 1.2 Hz, J_2 = 8.4 Hz, 2H, H-4′, H-6), 6.850 (d, J = 8.4 Hz, 2H, H-2′, H-5), 3.812 (s, 3H, 3-OCH_3), 2.893 (t, J = 5.4 Hz, 4H, 3″-CH_2, 5″-CH_2), 1.706-1.747 (m, 2H, 4″-CH_2). ESI-MS m/z: 338.4 $(M)^+$, calcd for $C_{21}H_{19}FO_3$: 338.1.

(2*E*,6*E*)-2-(4-Hydroxy-3-methoxybenzylidene)-6-(4-methoxybenzylidene)cyclohexanone (28): Green powder, 20.5% yield, mp 135.6-138.3°C. ^{1}H-NMR (d_6-DMSO) δ: 7.578 (d, J = 6.6 Hz, 2H, H-2′, H-6′), 7.522 (s, 1H, β'-H), 7.507 (s, 1H, β-H), 7.117 (s, 1H, H-2), 7.026 (t, J = 9.0 Hz, 3H, H-6, H-3′, H-5′), 6.851 (d, J = 8.4 Hz, 1H, H-5), 3.812 (s, 3H, 4′-OCH_3), 3.805 (s, 3H, 3-OCH_3), 2.863-2.909 (m, 4H, 3″-CH_2, 5″-CH_2), 1.704-1.745 (m, 2H, 4″-CH_2). ESI-MS m/z: 351.3 $(M+1)^+$, calcd for $C_{22}H_{22}O_4$: 350.2.

(2*E*,6*E*)-2-(2,4-Dimethoxybenzylidene)-6-(4-hydroxy-3-methoxybenzylidene)cyclohexanone (29): Yellow powder, 9.1% yield, mp 149.7-153.2°C. ^{1}H-NMR (d_6-DMSO) δ: 7.770 (s, 1H, β'-H), 7.554 (s, 1H, β-H), 7.340 (d, J = 9.0 Hz, 1H, H-6'), 7.113 (s, 1H, H-2), 7.035 (d, J = 8.4 Hz, 1H, H-6), 6.850 (d, J = 7.8 Hz, 1H, H-5), 6.627 (d, J = 1.8 Hz, 1H, H-3′), 6.594 (dd, J_1 = 2.4 Hz, J_2 = 9.0 Hz, 1H, H-5′), 3.836 (s, 3H, 3-OCH_3), 3.813 (s, 6H, 2′,5′-OCH_3), 2.770-2.901 (m, 4H, 3″-CH_2, 5″-CH_2), 1.692 (t, J = 5.4 Hz, 2H, 4''-CH_2). ESI-MS m/z: 381.0 $(M+1)^+$, calcd for $C_{23}H_{24}O_5$: 380.2.

(2*E*,6*E*)-2-(3,4-Difluorobenzylidene)-6-(4-hydroxy-3-methoxybenzylidene)cyclohexanone (30): Yellow powder, 8.1% yield, mp 172.1-174.2°C. ^{1}H-NMR (d_6-DMSO) δ: 7.561 (s, 2H, β'-H, β-H), 7.094-7.165 (m, 2H, H-2, H-6′), 7.033 (dd, J_1 = 1.2 Hz, J_2 = 7.8 Hz, 2H, H-2′, H-6), 6.850 (d, J = 8.4 Hz, 2H, H-5, H-5′), 3.812 (s, 3H, 3-OCH_3), 2.894 (t, J = 5.4 Hz, 4H, 3″-CH_2, 5″-CH_2), 1.706-1.747 (m, 2H, 4″-CH_2). ESI-MS m/z: 356.9 $(M+1)^+$, calcd for $C_{21}H_{18}F_2O_3$: 356.1.

(2*E*,6*E*)-2-(2,3-dichlorobenzylidene)-6-(4-hydroxy-3-methoxybenzylidene)cyclohexanone (31): Yellow powder, 25.3% yield, mp 169.7-171.9°C. ^{1}H-NMR (d_6-DMSO) δ: 7.560 (s, 2H, β'-H, H-4′), 7.112 (s, 2H, β-H, H-2), 7.032 (d, J = 8.4 Hz, 2H, H-5', H-6′), 6.848 (d, J = 8.4 Hz, 2H, H-5, H-6), 3.811 (s, 3H, 3-OCH_3), 2.893 (t, J = 5.4 Hz, 4H, 3″-CH_2, 5″-CH_2), 1.707-1.747 (m, 2H, 4″-CH_2). ESI-MS m/z: 388.9 $(M+1)^+$, calcd for $C_{21}H_{18}Cl_2O_3$: 388.1.

(2*E*,6*E*)-2-(4-Hydroxy-3-methoxybenzylidene)-6-(4-hydroxybenzylidene)cyclohexanone (32): Yellow powder, 16.0% yield, mp 168.5-171.0°C. ^{1}H-NMR (d_6-DMSO) δ: 7.560 (s, 1H, β'-H), 7.544 (s, 1H, β-H), 7.410 (d, J = 8.4 Hz, 2H, H-2′, H-6′), 7.113 (s, 1H, H-2), 7.023-7.040 (m, 2H, H-5, H-6), 6.850 (d, J = 8.4 Hz, 2H, H-3′, H-5'), 3.812 (s, 3H, 3-OCH_3), 2.893 (t, J = 5.4 Hz, 4H, 3″-CH_2, 5″-CH_2), 1.706-1.747 (m, 2H, 4″-CH_2). ESI-MS m/z: 336.9 $(M+1)^+$, calcd for $C_{21}H_{20}O_4$: 336.1.

(2*E*,6*E*)-2-(2,3-Dimethoxybenzylidene)-6-(4-hydroxy-3-methoxybenzylidene)cyclohexanone (33): Yellow powder, 4.2% yield, mp 147.2-150.0°C. ^{1}H-NMR (d_6-DMSO) δ: 7.561 (s, 2H, β-H, β'-H), 7.115 (d, J = 1.8 Hz, 2H, H-2, H-6'), 7.032 (dd, J_1 = 1.8 Hz, J_2 = 8.4 Hz, 2H, H-5′, H-6), 6.850 (d, J = 7.8 Hz, 2H, H-4′, H-5), 3.811 (s, 9H, 3-OCH_3, 2′,3′-OCH_3), 2.894 (t, J = 5.4 Hz, 4H, 3″-CH_2, 5″-CH_2), 1.706-1.747 (m, 2H, 4''-CH_2). ESI-MS m/z: 381.1 $(M+1)^+$, calcd for $C_{23}H_{24}O_5$: 380.2.

(2*E*,6*E*)-2-(4-Hydroxy-3-methoxybenzylidene)-6-(2-(trifluoromethyl)benzylidene)cyclohexanone (34): Yellow powder, 5.7% yield, mp 170.4-172.2°C. ^{1}H-NMR (d_6-DMSO) δ: 7.450-7.670 (m, 3H, β-H, β'-H, H-3′), 7.084-7.121 (m, 3H, H-4′, H-5′, H-6′), 7.114 (s, 1H, H-2), 7.032 (dd, J_1 = 1.2 Hz, J_2 = 8.4 Hz, 1H, H-6), 6.849 (d, J = 7.8 Hz, 1H, H-5), 3.811 (s, 3H, 3-OCH_3), 2.893 (t, J = 5.4 Hz, 4H, 3″-CH_2, 5″-CH_2), 1.706-1.746 (m, 2H, 4″-CH_2). ESI-MS m/z: 388.9 $(M+1)^+$, calcd for $C_{22}H_{19}F_3O_3$: 388.1.

(2*E*,6*E*)-2-(2,6-Difluorobenzylidene)-6-(4-hydroxy-3-methoxybenzylidene)cyclohexanone (35): Brown yellow powder, 9.0% yield, mp 160.2-162.1°C. ^{1}H-NMR (d_6-DMSO) δ: 7.545 (s, 2H, β'-H, β-H), 7.098 (d, J = 8.4 Hz, 2H, H-6, H-4′), 7.016 (dd, J_1 = 1.2 Hz, J_2 = 8.4 Hz, 2H, H-2, H-5), 6.833 (d, J = 8.4 Hz, 2H, H-3′, H-5′), 3.795 (s, 3H, 3-OCH_3), 2.878 (t, J = 5.4 Hz, 4H, 3″-CH_2, 5″-CH_2), 1.691-1.731 (m, 2H, 4″-CH_2). ESI-MS m/z: 356.9 $(M+1)^+$, calcd for $C_{21}H_{18}F_2O_3$: 356.1.

(2*E*,6*E*)-2-(3,4-Dichlorobenzylidene)-6-(4-hydroxy-3-methoxybenzylidene)cyclohexanone (36): Yellow powder, 14.1% yield, mp 140.1-142.6°C. ^{1}H-NMR (d_6-DMSO) δ: 7.647 (d, J = 8.4 Hz, 1H, H-6′), 7.584 (d, J = 1.8 Hz, 1H, H-2′), 7.561 (s, 2H, β'-H, β-H), 7.379 (d, J = 7.8 Hz, 1H, H-5′), 7.115 (d, J = 1.8 Hz, 1H, H-2,), 7.032 (dd, J_1 = 1.8 Hz, J_2 = 8.4 Hz, 1H, H-5), 6.850 (d, J = 7.8 Hz, 1H, H-6), 3.812 (s, 3H, 3-OCH_3), 2.894 (t, J = 5.4 Hz, 4H, 3″-CH_2, 5″-CH_2), 1.707-1.748 (m, 2H, 4″-CH_2). ESI-MS m/z: 389.1 $(M+1)^+$, calcd for $C_{21}H_{18}Cl_2O_3$: 388.1.

(2*E*,6*E*)-2-(5-Bromo-2-ethoxybenzylidene)-6-(4-hydroxy-3-methoxybenzylidene)cyclohexanone (37): Yellow powder, 12.2% yield, mp 118.3-120.2°C. ^{1}H-NMR (d_6-DMSO) δ: 7.663 (s, 1H, H-6'), 7.582 (s, 1H, β'-H), 7.511 (dd, J_1 = 2.4 Hz, J_2 = 8.4 Hz, 1H, H-4'), 7.326 (s, 1H, β-H), 7.127 (d, J = 1.8 Hz, 1H, H-2), 7.043 (d, J = 9.0 Hz, 2H, H-5, H-6), 6.843 (d, J = 8.4 Hz, 1H, H-3′), 4.090 (q, J = 7.2 Hz, 2H, -OC$\underline{H_2}$$CH_3$), 3.814 (s, 3H, 3-$OCH_3$), 2.879-2.915 (m, 4H, 3″-CH_2, 5″-CH_2), 1.689-1.729 (m, 2H, 4″-CH_2), 1.343 (t, J = 5.4 Hz, 3H, -$OCH_2C\underline{H_3}$). ESI-MS m/z: 443.5 $(M+1)^+$, calcd for $C_{23}H_{23}BrO_4$: 442.1.

4.2 Animals

Sprague-Dawley (SD) rats aged 6 weeks, 180–220 g, were obtained from the Animal Center of Wenzhou Medical University (Wenzhou, China). Rats were kept in a constant room temperature with a 12:12 hours light-dark cycle and fed with a standard rodent diet and water. Before experiments, the rats were acclimatized to the laboratory for at least 7 days. Protocols involving the use of animals were approved by the Wenzhou Medical College Animal Policy and Welfare Committee (Approval documents: wydw2014-0093).

4.3 Cells and reagents

RAW 264.7 macrophages, human normal hepatic cell HL-7702 and human lung epithelial BEAS-2B were obtained from Shanghai Institute of Biosciences and Cell Resources Center (Chinese Academy of Sciences, Shanghai, China). Cells were incubated in RPMI 1640 medium (Gibco®, life Technologies, Carlsbad, VA, USA) supplemented with 10% fetal bovine serum (Gibco®, life Technologies, Carlsbad, VA, USA), 100 U/mL penicillin, and 100 mg/mL streptomycin at 37 °C with 5% CO_2. LPS purchased from

Sigma (Sigma, St Louis, MO, USA) was dissolved in PBS. DMSO is the vehicle and used for dissolving the synthesized ScMACs.

4.4 Determination of TNF-α and IL-6

RAW264.7 macrophages were pretreated with the corresponding amount of ScMAC for 30 mins, followed by LPS (0.5 μg/mL) stimulation for 24 h. The culture media and cells were collected. TNF-α and IL-6 levels in the medium were determined with an ELISA kit (eBioScience, Inc.) according to the manufacturer's instruction. The total amount of the inflammatory factor in the medium was normalized to the total protein quantity of the viable cell pellets.

4.5 MTT (methyl thiazolyl tetrazolium) assay

HL-7702 cells were seeded into 96-well plates at a density of 5000 cells per well in 1640 medium, supplemented with 10% heat-inactivated serum, 100 U/mL penicillin, and 100 μg/mL streptomycin. The cells were incubated at 37 °C in a humidified atmosphere containing 5% CO_2 for 24 h. Tested compounds were dissolved in DMSO and diluted with 1640 medium to the final concentrations of 10 μM. Then, the cells were refilled with the medium with test compounds for another 24 hours before the MTT assay. Fresh solution of MTT (20 μL, 5 mg/mL) prepared in PBS was added to each single well of the 96-well plate. The plates were then incubated in a CO_2 incubator for 4 hours. Finally, cells were dissolved with 150 μL DMSO and then analyzed in a multi-well-plate reader at 490 nm.

4.6 LPS-induced ALI in rats

The 18 male SD rats were randomly divided into three groups on average, including control group, LPS group, and **6** + LPS group. The rats in **6** + LPS group orally received **6** (20 mg/kg/day) in 0.5% Carboxymethylcellulose Sodium (CMCNa) solution for 7 days before administration of LPS. Rats from control and LPS groups received equal volume of 0.5% CMCNa. After being anesthetized by diethyl ether, rats from LPS group and **6** + LPS group were intratracheal-instilled 50 μL LPS (5 mg/kg) to induce lung injury. Control rats were given 50 μL physiological saline solutions. Six hours after LPS administration, rats were given anesthesia by intraperitoneal injection of 10% chloral hydrate solution (5 mL/kg). The right lung of all rats were lavaged with 1 mL physiological saline three times. Collection of BALF solution was used for further study.

4.7 Determination total protein concentration, number of neutrophils, and relative amount of TNF-α in BALF

BALF cells and supernatant were separated by centrifugal separation at 4 °C. Total protein concentration in supernatant of BALF was measured using a bicinchoninic acid (BCA) assay kit according to the manufacturer's instructions, with bovine serum albumin (BSA) as the standard. The cells of BALF were resuspended in 50 μL physiological saline and used for neutrophils cell counts by Wright-Giemsa stain. Relative amount of TNF-α in supernatant of BALF was determined with an ELISA kit as above.

4.8 Lung Wet-to-Dry Weight (W/D) ratio measurement

Superior lobes of right lungs were excised, blotted dry, and weighed to obtain the "wet" weight. Then the lungs were placed in an oven at 60 °C for more than 48 h until getting constant weight as dry weight. The ratio of the wet lung to the dry lung was calculated to assess tissue edema.

4.9 Histopathologic evaluation

Lung tissues abtained from above were washed with PBS solution, blotted dry, fixed with 4% paraformaldehyde, embedded in paraffin and sectioned (5 μm). After H&E staining and CD68 staining, pathological changes in the lung tissues were observed under a light microscope.

4.10 Real-time quantitative PCR

Tissue and cells were homogenized in TRIZOL kit (Invitrogen, Carlsbad, CA) for extraction of RNA according to each manufacturer's protocol. Both reverse transcription and quantitative PCR were carried out using a two-step M-MLV Platinum SYBR Green qPCR SuperMix- UDG kit (Invitrogen, Carlsbad, CA). Eppendorf Mastercycler ep realplex detection system (Eppendorf, Hamburg, Germany) was used for q-PCR analysis. The primers of genes were synthesized by Invitrogen. The primer sequences of mouse genes used are shown as follows:

Rat TNF-α sense: 5′-TACTCCCAGGTTCTCTTCAAGG-3′;

Rat TNF- α antisense: 5′-GGAGGCTGACTTTCTCCTGGT A-3′;

Rat IL-6 sense: 5′-GAGTTGTGCAATGGCAATTC-3′;

Rat IL-6 antisense: 5′-ACTCCAGAAGACCAGAGCAG-3′;

Rat IL-1β sense: 5′-CACCTCTCAAGCAGAGCACAG-3′

Rat IL-1β antisense: 5′-GGGTTCCATGGTGAAGTCAAC-3′;

Rat COX-2 sense 5′-CGGAGGAGAAGTGGGGTTTAGGAT -3′;

Rat COX-2 antisense: 5′-TGGGAGGCACTTGCGTTGATGG -3′.

Rat ICAM-1 sense: 5′-AGATCATACGGGTTTGGGCTTC-3′

Rat ICAM-1 antisense: 5′-TATGACTCGTGAAAGAAATCA GCTC-3′;

Rat VCAM-1 sense 5′-TTTGCAAGAAAAGCCAACATGA AAG-3′;

Rat VCAM-1 antisense: 5′-TCTCCAACAGTTCAGACGTTA GC-3′.

Rat actin sense: 5′-AAGTCCCTCACCCTCCCAAAAG-3′;

Rat actin antisense: 5′-AAGCAATGCTGTCACCTTCCC-3′;

Human TNF-α sense: 5′-CCCAGGGACCTCTCTCTAATC-3′;

Human TNF-α antisense: 5′-ATGGGCTACAGGCTTGTCA CT-3′;

Human IL-6 sense: 5′-GCACTGGCAGAAAACAACCT-3′;

Human IL-6 antisense: 5′-TCAAACTCCAAAAGACCAGTG A-3′;

Human IL-1β sense: 5′-ACGCTCCGGGACTCACAGCA-3′

Human IL-1β antisense: 5′-TGAGGCCCAAGGCCACAGG T-3′;

Human COX-2 sense 5′-TTCTCCTTGAAAGGACTTATGG GTAA-3′;

Human COX-2 antisense: 5′-AGAACTTGCATTGATGGTG ACTGTTT-3′.

Human actin sense: 5′-CCTGGCACCCAGCACAAT-3′;

Human actin antisense: 5′-GCCGATCCACACGGAGTACT-3′;

The amount of each gene was determined and normalized by the amount of β-actin.

Acknowledgments

Financial support was provided by the National Natural Science Funding of China (21272179 and 81272462), Project of Zhejiang Provincial Key Constructive Subject (Traditional Chinese Medicine, 2012-XK-A28), Zhejiang Natural Science Funding (LQ14H310003), and Zhejiang College Students' Science and Technology Innovation Activities Program (2014R413071).

Notes and references

[a] Chemical Biology Research Center, School of Pharmaceutical Sciences, Wenzhou Medical University, Wenzhou, Zhejiang 325035, China.
[b] The 2nd Affiliated Hospital, Wenzhou Medical University, Wenzhou, Zhejiang 325035, China,
[c] The children's hospital, Zhejiang University School of Medicine, Hangzhou, Zhejiang 310003, China.
[d] School of Laboratory Medicine and Life Science, Wenzhou Medical University, Wenzhou, Zhejiang 325035, China.
† These authors contribute equally to this work.
* Corresponding author, Tel.: +86 577 86699524; fax: +86 577 86699527 (G.L.) e-mail: chemime@163.com (P, Feng), wzmcliangguang @163.com (G. liang)

1. L. B. Ware, M. A. Matthay, The acute respiratory distress syndrome, *N. Engl. J. Med.* 2000, **342**, 1334-1349.
2. K. Tsushima, L. S. King, N. R. Aggarwal, A. De Gorordo, F. R. D'Alessio, *Acute lung injury review, Intern. Med.* 2009, **48**, 621-630.
3. F. Frutos-Vivar, N. Nin, A. Esteban, Epidemiology of actue lung injury and acute respiratory distress syndrome, *Curr. Opin. Crit. Care,* 2004, **10**, 1-6.
4. G. D. Rubenfeld, E. Caldwell, E. Peabody, J. Weaver, D. P. Martin, M. Neff, E. J. Stern, L. D. Hudson, Incidence and outcomes of acute lung injury**,** *N. Engl. J. Med.* 2009, **353**, 1685-1693.
5. M. R. Hemmila, L. M. Napolitano, Severe respiratory failure: advanced treatment options**,** *Critical Care Medicine*, 2006, **34**, S278-S290.
6. R. B. Goodman, J. Pugin, J. S. Lee, M. A. Matthay, Cytokine-mediated inflammation in acute lung injury, *Cytokine Growth Factor Rev*. 2003, **14**, 523-535.
7. M. Bhatia, S. Moochhala, Role of inflammatory mediators in the pathophysiology of acute respiratory distress syndrome**,** *J. Pathol*. 2004, **202**, 145-156.
8. G. U. Meduri, G. Kohler, S. Headley, E. Tolley, F. Stentz, A. Postlethwaite, Inflammatory cytokines in the BAL of patients with ARDS. Persistent elevation over time predicts poor outcome, *Chest,* 1995, **108**, 1303-1314.
9. S. Mukhopashyay, J. R. Hoidal, T. K. Mukherjee, Role of TNFalpha in pulmonary pathophysiology, *Respir Res.* 2006, **7**, 125.
10. L. I. Schrader, D. W. Kinzenbaw, A. W. Johnson, F. W. Faraci, S. P. Didion, IL-6 deficiency protects against angiotensin II induced endothelial dysfunction and hypertrophy, Arteriosclerosis, *thrombosis, and vascular biology*, 2007, **27**, 2576-2581.
11. X. Zhang, J. Hou, X. Qin, W Li, H Chen, R. Liu, X Liang, C. Hai, Pentoxifylline inhibits intercellular adhesion molecule-1 (ICAM-1) and lung injury in experimental phosgene-exposure rats, *Inhal Toxicol*, 2010, **22**, 889-895.
12. R. B. Goodmana, Jérˆome Pugin, J. S. Lee, M. A. Matthay, Cytokine-mediated inflammation in acute lung injury. *Cytokine Growth F R.* 2003, **14**, 523-535.
13. T. Schorn, F. Drago, G. Tettamanti, R. Valvassori, M. de Eguileor, J. Vizioli, A. Grimaldi, Homolog of allograft inflammatory factor-1 induces macrophage migration during innate immune response in leech. *Cell Tissue Res*. 2015, **359**, 853-864.
14. R. K. Maheshwari, A. K. Singh, J. Gaddipati, R. C. Srimal, Multiple biological activities of curcumin: a short review, *Life Sci.* 2006, **78**, 2081-2087.
15. I. Chattopadhyay, K. Biswas, U. Bandyopadhyay, R. K. Banerjee, Turmeric and curcumin: Biological actions and medicinal applications, *Curr. Sci.* 2004, **87**, 44-53.
16. T. Esatbeyoglu, P. Huebbe, I. M. A. Ernst, D. China, A. E. Wagner, G. Rimbach, **C**urcumin-from molecule to biological function, *Angew. Chem. Int. Ed.* 2012, **51**, 5308-5332.
17. B. B. Aggarwal, C. Sundaram, N. Malani, H. Ichikawa, Curcumin: the indian solid gold, *Advan. Exp. Med. Biol.* 2007, **595**, 1-75.
18. V. P. Kurup, C. S. Barrios, Immunomodulatory effects of curcumin in allergy, *Mol. Nutr. Food Res.* 2008, **52**, 1031-1039.
19. K. Nakamura, Y. Yasunaga, T. Segawa, D. Ko, J. W. Moul, S. Srivastava, J. S. Rhim, Curcumin down-regulates AR gene expression and activation in prostate cancer cell lines, *Int. J. Oncol.* 2002, **21**, 825-830.
20. C. H. Hsu, A. L. Cheng, Clinical studies with curcumin. *Adv Exp Med Biol*, 2007, **595**, 471-80.
21. A. L. Cheng, C. H. Hsu, J. K. Lin, M. M. Hsu, Y. F. Ho, T. S. Shen, J. Y. Ko, J. T. Lin, B. R. Lin, W. Ming-Shiang, H. S. Yu, S. H. Jee, G. S. Chen, T. M. Chen, C. A. Chen, M. K. Lai, Y. S. Pu, M. H. Pan, Y. J. Wang, C. C. Tsai, C. Y. Hsieh, Phase I clinical trial of curcumin, a chemopreventive agent, in patients with high-risk or pre-malignant lesions, *Anticancer Res.* 2001, **21**, 2895-900.
22. X. Xiao, M. Yang, D. Sun, S. Sun, Curcumin protects against sepsis-induced acute lung injury in rats, *J. Surg. Res.* 2012, **176**, e31-39.
23. S. Bansal, S. Chhibber, Curcumin alone and in combination with augmentin protects against pulmonary inflammation and acute lung injury generated during Klebsiella pneumonia B5055-induced lung infection in BALB/c mice, *J. Med. Microbiol*. 2010, **59**, 429-437.
24. P. Anand, A. B. Kunnumakkara, R. A. Newman, B. B. Aggarwal, Bioavailability of curcumin: problems and promises, *Mol. Pharm.* 2007, **4**, 807-818.
25. M. H. Pan, T. M. Huang, J. K. Lin, Biotransformation of curcumin through reduction and glucuronidation in micse, *Drug Metab. Dispos.* 1999, **27**, 486–494.
26. M. J. Rosemond, L. St. John-Williams, T. Yamaguchi, T. Fujishita, J. S. Walsh, Enzymology of a carbonyl reduction clearance pathway for the HIV integrase inhibitor, S-1360: Role of human liver cytosolic aldo-keto reductases, *Chem.-Biol. Interact.* 2004, **147**, 129–139.
27. G. Grogan, Emergent mechanistic diversity of enzyme-catalysed beta-diketone cleavage, *Biochem. J.* 2005, **388**, 721–730.
28. Z. Liu, L. Tang, P. Zou, Y. Zhang, Z. Wang, Q. Fang, L. Jiang, G. Chen, Z. Xu, H. Zhang, G. Liang, Synthesis and biological evaluation of allylated and prenylated mono-carbonyl analogs of curcumin as anti-inflammatory agents, *Eur J. Med. Chem.* 2014, **74**, 671-682.
29. C. Zhao, Y. Cai, X. He, J. Li, L. Zhang, J. Wu, Y. Zhao, S. Yang, X. Li, W. Li, G. Liang, Synthesis and anti-inflammatory evaluation of novel mono-carbonyl analogues of curcumin in LPS-stimulated RAW 264.7 macrophages, *Eur J. Med. Chem.* 2010, **45**, 5773-5780.
30. G. Liang, S. Yang, H. Zhou, L. Shao, K. Huang, J. Xiao, Z. Huang, X. Li, Synthesis, crystal structure and anti-inflammatory properties of curcumin analogues, *Eur J. Med. Chem.* 2009, **44**, 915-919.
31. G. Liang, X. Li, L. Chen, S. Yang, X. Wu, E. Studer, E. Gurley, P. B. Hylemon, F. Ye, Y. Li, H. Zhou, Synthesis and anti-inflammatory activities of mono-carbonyl analogues of curcumin, *Bioorg. Med. Chem. Lett.* 2008, **18**, 1525-1529.
32. G. Liang, L. Shao, Y. Wang, C. Zhao, Y. Chu, J. Xiao, Y. Zhao, X. Li, S. Yang, Exploration and synthesis of curcumin analogues with improved structural stability both *in vitro* and *in vivo* as cytotoxic agents, *Bioorg. Med. Chem.* 2009, **17**, 2623–2631.
33. Y. Wang, C. Yu, Y. Pan, J. Li, Y. Zhang, F. Ye, S. Yang, H. Zhang, X. Li, G. Liang, A novel compound C12 inhibits inflammatory cytokine production and protects from inflammatory injury *in vivo*, *PLoS ONE*, 2011, **6**, e24377- e24377.
34. Y. L. Zhang, L. P. Zhao, J. Z. Wu, X. Jiang, L. L. Dong, F. L. Xu, P. Zou, Y. R. Dai, X. O. Shan, S. L. Yang, G. Liang, Synthesis and evaluation of a series of novel asymmetrical curcumin analogs for the treatment of inflammation, *Molecules*, 2014, **19**, 7287-7307.
35. H. E. Marshall, E. N. Potts, Z. T. Kelleher, J. S. Stamler, W. M. Foster, R. L. Auten, Protection from lipopolysaccharide-induced lung injury by

augmentation of airway S-nitrosothiols, *Am. J. Respir. Crit. Care Med.* 2009, **180**, 11-18.
36. W. Y. Shao, Y. N. Cao, Z.W. Yu, W. J. Pan, X. Qiu, X. Z. Bu, L. K. An, Z. S. Huang, L. Q. Gu, Albert S. C. Chan, Facile preparation of new unsymmetrical curcumin derivatives by solid-phase synthesis strategy, *Tetrahedron Lett.* 2006, **47**, 4085-4089.

